The Holocene

http://hol.sagepub.com/

A database and synthesis of northern peatland soil properties and Holocene carbon and nitrogen accumulation

Julie Loisel, Zicheng Yu, David W Beilman, Philip Camill, Jukka Alm, Matthew J Amesbury, David Anderson, Sofia Andersson, Christopher Bochicchio, Keith Barber, Lisa R Belyea, Joan Bunbury, Frank M Chambers, Daniel J Charman, François De Vleeschouwer, Barbara Fialkiewicz-Koziel, Sarah A Finkelstein, Mariusz Galka, Michelle Garneau, Dan Hammarlund, William Hinchcliffe, James Holmquist, Paul Hughes, Miriam C Jones, Eric S Klein, Ulla Kokfelt, Atte Korhola, Peter Kuhry, Alexandre Lamarre, Mariusz Lamentowicz, David Large, Martin Lavoie, Glen MacDonald, Gabriel Magnan, Markku Mäkilä, Gunnar Mallon, Paul Mathijssen, Dmitri Mauquoy, Julia McCarroll, Tim R Moore, Jonathan Nichols, Benjamin O'Reilly, Pirita Oksanen, Maara Packalen, Dorothy Peteet, Pierre JH Richard, Stephen Robinson, Tiina Ronkainen, Mats Rundgren, A Britta K Sannel, Charles Tarnocai, Tim Thom, Eeva-Stiina Tuittila, Merritt Turetsky, Minna Väliranta, Marjolein van der Linden, Bas van Geel, Simon van Bellen, Dale Vitt, Yan Zhao and Weijian Zhou

The online version of this article can be found at:
http://hol.sagepub.com/content/early/2014/07/02/0959683614538073

Published by:

$SAGE

http://www.sagepublications.com

Additional services and information for *The Holocene* can be found at:

Email Alerts: http://hol.sagepub.com/cgi/alerts

Subscriptions: http://hol.sagepub.com/subscriptions

Reprints: http://www.sagepub.com/journalsReprints.nav

Permissions: http://www.sagepub.com/journalsPermissions.nav

Citations: http://hol.sagepub.com/content/early/2014/07/02/0959683614538073.refs.html

>> OnlineFirst Version of Record - Jul 3, 2014

What is This?
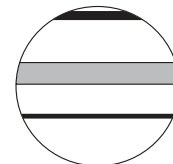
A database and synthesis of northern peatland soil properties and Holocene carbon and nitrogen accumulation

Julie Loisel,[1] Zicheng Yu,[1] David W Beilman,[2] Philip Camill,[3] Jukka Alm,[4] Matthew J Amesbury,[5] David Anderson,[6] Sofia Andersson,[7] Christopher Bochicchio,[1] Keith Barber,[8] Lisa R Belyea,[9] Joan Bunbury,[10] Frank M Chambers,[11] Daniel J Charman,[5] François De Vleeschouwer,[12] Barbara Fiałkiewicz-Kozieł,[13] Sarah A Finkelstein,[14] Mariusz Gałka,[13] Michelle Garneau,[15] Dan Hammarlund,[16] William Hinchcliffe,[5] James Holmquist,[17] Paul Hughes,[8] Miriam C Jones,[18] Eric S Klein,[1] Ulla Kokfelt,[19] Atte Korhola,[20] Peter Kuhry,[7] Alexandre Lamarre,[15] Mariusz Lamentowicz,[13] David Large,[21] Martin Lavoie,[22] Glen MacDonald,[17] Gabriel Magnan,[15] Markku Mäkilä,[23] Gunnar Mallon,[8] Paul Mathijssen,[20] Dmitri Mauquoy,[24] Julia McCarroll,[11] Tim R Moore,[25] Jonathan Nichols,[26] Benjamin O'Reilly,[14] Pirita Oksanen,[27] Maara Packalen,[28] Dorothy Peteet,[26] Pierre JH Richard,[29] Stephen Robinson,[30] Tiina Ronkainen,[20] Mats Rundgren,[16] A Britta K Sannel,[7] Charles Tarnocai,[31] Tim Thom,[32] Eeva-Stiina Tuittila,[4] Merritt Turetsky,[33] Minna Väliranta,[20] Marjolein van der Linden,[34] Bas van Geel,[35] Simon van Bellen,[23] Dale Vitt,[36] Yan Zhao[37] and Weijian Zhou[38]

Abstract

Here, we present results from the most comprehensive compilation of Holocene peat soil properties with associated carbon and nitrogen accumulation rates for northern peatlands. Our database consists of 268 peat cores from 215 sites located north of 45°N. It encompasses regions within which peat carbon data have only recently become available, such as the West Siberia Lowlands, the Hudson Bay Lowlands, Kamchatka in Far East Russia, and the Tibetan Plateau. For all northern peatlands, carbon content in organic matter was estimated at 42 ± 3% (standard deviation) for *Sphagnum* peat, 51 ± 2% for non-*Sphagnum* peat, and at 49 ± 2% overall. Dry bulk density averaged 0.12 ± 0.07 g/cm^3, organic matter bulk density averaged 0.11 ± 0.05 g/cm^3, and total carbon content in peat averaged 47 ± 6%. In general, large differences were found between *Sphagnum* and non-*Sphagnum* peat types in terms of peat properties. Time-weighted peat carbon accumulation rates averaged 23 ± 2 (standard error of mean) g C/m^2/yr during the Holocene on the basis of 151 peat cores from 127 sites, with the highest rates of carbon accumulation (25–28 g C/m^2/yr) recorded during the early Holocene when the climate was

[1]Lehigh University, USA
[2]University of Hawaii – Manoa, USA
[3]Bowdoin College, USA
[4]University of Eastern Finland, Finland
[5]University of Exeter, UK
[6]Eton College, UK
[7]Stockholm University, Sweden
[8]University of Southampton, UK
[9]Queen Mary University of London, UK
[10]University of Wisconsin – La Crosse, USA
[11]University of Gloucestershire, UK
[12]CNRS and Université de Toulouse, France
[13]Adam Mickiewicz University, Poland
[14]University of Toronto, Canada
[15]Université du Québec – Montréal, Canada
[16]Lund University, Sweden
[17]University of California – Los Angeles, USA
[18]U.S. Geological Survey, USA
[19]University of Copenhagen, Denmark
[20]University of Helsinki, Finland
[21]University of Nottingham, UK
[22]Université Laval, Canada
[23]Geological Survey of Finland, Finland
[24]University of Aberdeen, UK

[25]McGill University, Canada
[26]Columbia University, USA
[27]Centre for Economic Development, Transport and the Environment, Finland
[28]University of Toronto, Canada
[29]Université de Montréal, Canada
[30]Champlain College – Dublin Campus, Ireland
[31]Agriculture and Agri-Food Canada, Canada
[32]Yorkshire Peat Partnership, Yorkshire Wildlife Trust, UK
[33]University of Guelph, Canada
[34]BIAX Consult, The Netherlands
[35]University of Amsterdam, The Netherlands
[36]Southern Illinois University, USA
[37]Chinese Academy of Sciences, China
[38]Chinese Academy of Sciences, China

Corresponding authors:
Julie Loisel, Department of Earth and Environmental Sciences, Lehigh University, Bethlehem, PA 18015, USA.
Email: jul208@lehigh.edu

Zicheng Yu, Department of Earth and Environmental Sciences, Lehigh University, Bethlehem, PA 18015, USA.
Email: ziy2@lehigh.edu

warmer than the present. Furthermore, we estimate the northern peatland carbon and nitrogen pools at 436 and 10 gigatons, respectively. The database is publicly available at https://peatlands.lehigh.edu.

Introduction

Of all terrestrial ecosystems, peatlands are arguably the most efficient at sequestering carbon (C) over long time scales. Northern peatlands cover approximately 4,000,000 km^2 or 3% of the global land area (Maltby and Immirzi, 1993) and have accumulated about 500 gigatons of C (GtC) mostly during the Holocene, equivalent to ~30% of the present-day global soil organic carbon (SOC) pool (Bridgham et al., 2006; Gorham, 1991; Yu et al., 2010). These ecosystems have also played a dynamic role in the Holocene global C cycle as important sinks of carbon dioxide (CO$_2$) and major sources of methane (CH$_4$) to the atmosphere (Frolking and Roulet, 2007; Korhola et al., 2010; Yu, 2011). As climate warming positively affects both plant growth and organic matter (OM) decomposition, recent and projected climate change could shift the balance between peat production and OM decomposition, potentially affecting the peatland C-sink capacity and modifying peat C fluxes to the atmosphere (Frolking et al., 2011; Yu, 2012). This prediction particularly holds true for the northern high-latitude regions, where the intensity of climate change is expected to be greatest (McGuire et al., 2009). The peatland C cycle–climate feedback remains difficult to assess, however, because of (1) limited understanding of peatland responses to climate change (Frolking et al., 2011), (2) data gaps and large uncertainties in regional peatland C stocks (Yu, 2012), and (3) non-linear peatland responses to external forcing (Belyea, 2009).

Very little is known about the nitrogen (N) budget that accompanies C accumulation in northern peatlands (but see Limpens et al. (2006) for a review). Assuming a net C sequestration of ~270 GtC (Yu, 2012) and a C/N ratio of 20–30 for fen peat (Bergner et al., 1990; Rydin and Jeglum, 2013; results therein) during the early Holocene (11–7 kyr), about 10–13 GtN would have been required to build such peat deposits. It is therefore possible that northern peatlands have been playing an undocumented, dynamic role in the Holocene global N cycle as important sinks of N, potentially limiting the amount of N available for other ecosystems at the global scale (McLauchlan et al., 2013). Alternatively, if the main N input to peatlands was through N$_2$ fixation by bacteria, these microorganisms might have been more important in driving the C cycle in peatlands than previously thought. Overall, studying the coupling between N and C cycling in northern peatlands is essential for a better understanding of how key biogeochemical processes interact in these systems and for predicting the fate of peat C stocks.

Here, we present the most comprehensive compilation of Holocene C and N data for northern peatlands. This synthesis encompasses regions within which peat C and N data have only recently become available, such as the West Siberian Lowlands in Asian Russia, the Hudson Bay Lowlands in Canada, Kamchatka in the Russian Far East, and the Tibetan Plateau in China. In addition, we present the most comprehensive synthesis of peat soil properties (such as bulk density (BD), OM content (OM%), C and N content) from the northern hemisphere. Also, this new database and synthesis work represent a major expansion from Yu et al.'s (2009) synthesis on Holocene peat C dynamics, which was based on 33 sites (vs 127 sites as reported in this paper). Finally, it constitutes a natural continuation of Charman et al.'s (2013) recent study on peat C accumulation in northern peatlands during the last millennium.

In addition to filling regional data and knowledge gaps, the main objectives of this paper are (1) to describe a database of peat soil properties and synthesize this information for different peat types, time intervals, and geographic regions and (2) to produce time series of Holocene peat C and N accumulation rates in 500-year bins for comparison with climate history. Key differences in Holocene peat properties between different regions and peatland types are also discussed in light of their implications for long-term peat C stocks. Of particular importance and relevance are the differences between *Sphagnum* and non-*Sphagnum* peat types. Finally, we present new estimates for northern peat C and N stocks for northern peatlands on the basis of the expanded database.

Database and analysis

Database

We compiled a dataset of 268 published and unpublished Holocene peat records from 215 sites located in North America and Eurasia (Figure 1; Supplementary Table S1, available online). The difference in the number of peat cores and peatland sites is because of the fact that, in a few instances, multiple cores were collected from a single peatland. As these multiple cores were not designed as true replicates in the original publications, each of these cores was considered as an independent record of peat properties in this study. However, only the oldest core for each site was used for estimating peat inception age. Finally, when calculating peat C accumulation rates from a subset of 127 sites, multiple cores from a single site were each attributed an equal fraction of the weight for that site. For example, for a site with three cores, the peat C accumulation history of each core only accounted for 1/3 of the site's record.

The latitude of most peatland sites ranges from 45° to 69°N. The cutoff at 45°N represents the southern limit for defining what is considered to be the area contributing to the C cycle of the Arctic region (McGuire et al., 2009). Four high-elevation sites found in China (the Tibetan Plateau) and Japan were also included, as they developed under similar 'northern' climatic conditions. The name and coordinates of these four sites are as follows: Zoige (33.5°N, 102.6°E), Hongyuan (32.8°N, 102.5°E), Hani (42.2°N, 126.5°E), and Utasai (42.4°N, 140.2 E). A total of 155 cores originate from Eurasia, including 112 cores from Russia. The remaining 113 cores come from North America. Approximately 40% of all cores were collected from ombrotrophic bogs (n = 110 cores) and 20% were extracted from minerotrophic fens (n = 50 cores). The remainder (40%) was collected in peatlands currently affected by permafrost (n = 108 cores). Note that peatland type was identified independently for each site by the original investigators. From an ecosystem functioning perspective, distinguishing bogs from fens and permafrost peatlands is important, as these peatland types are characterized by different hydrological regimes, vegetation communities, and peat-growth trajectories, all of which impact long-term rates of peat C sequestration (Rydin and Jeglum, 2013). Bogs are mineral-poor, rain-fed peatland ecosystems with relatively low plant net primary production (NPP) and slow peat decomposition rates. In contrast, fens are hydrologically
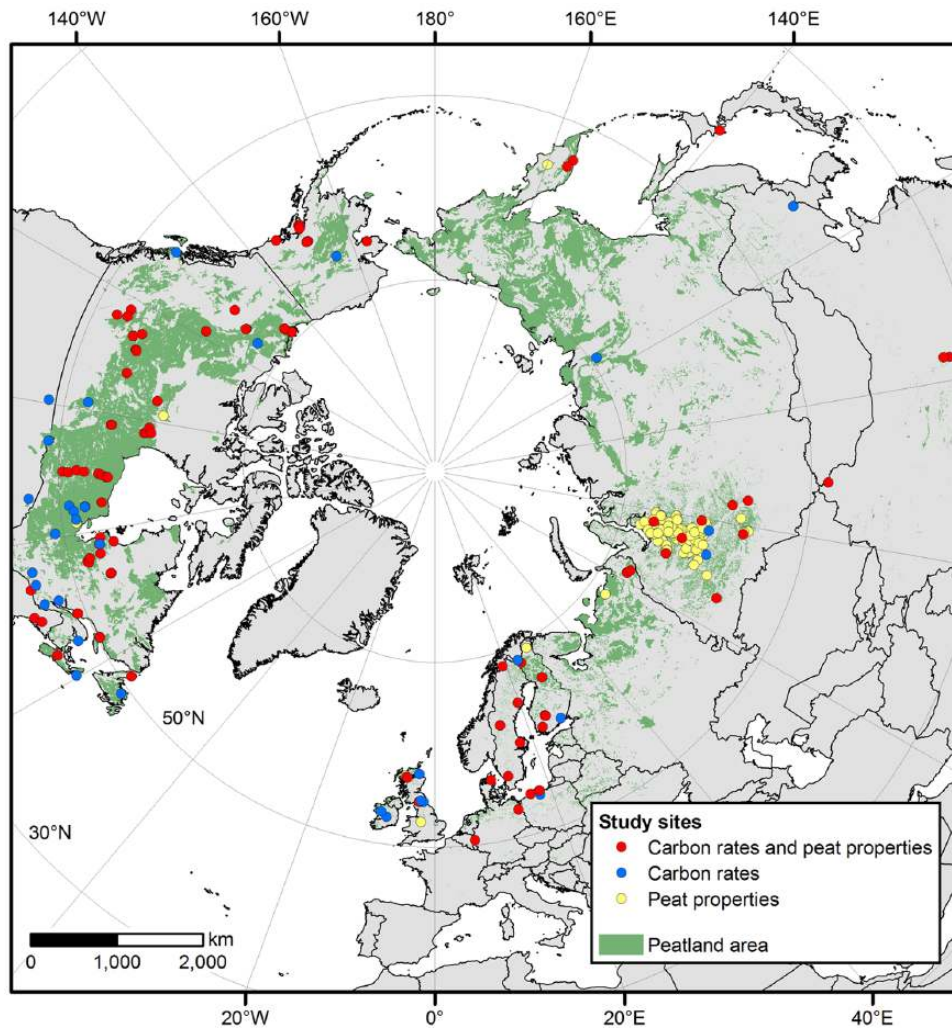
Figure 1. Location of study sites. Map showing the distribution of northern peatlands (green area from Yu et al., 2010) and peatland sites included in this study (*n* = 215 sites, including 268 peat cores). Long-term rate of peat carbon accumulation was estimated from 127 sites (151 peat cores; red and blue dots). The yellow dots represent cores for which only peat properties (bulk density, organic matter content, etc.) were available and synthesized. Refer to Supplementary Table S1 (available online) for details.

connected to surface or ground water, thereby receiving more mineral nutrients. Generally speaking, fens have greater NPP but also faster peat decay rates than bogs (Blodau, 2002). Finally, in the sub-Arctic and Arctic regions, peatland hydrology, structure, and peat C balance are sensitive to the underlying permafrost aggradation and degradation dynamics (Camill, 1999; Turetsky et al., 2007). For the analysis, peat plateaus (87 out of 108 cores), permafrost bogs (18 out of 108 cores), and collapse scars (3 out of 108 cores) were grouped under the peatland type 'permafrost peatlands'. Original peatland categories can be found in Supplementary Table S1 (available online).

The database was built to include as many peat records as possible. Therefore, we included any peat core that was extracted north of 45°N (or at high elevation) and for which BD or OMBD data were available. Information related to peat-core location, peatland type, peat properties, age, and data source can be found in Supplementary Table S1 (available online). Additional information related to the type of coring device used and the year of coring can be found in the original publications. Data used in this synthesis are readily accessible from the Holocene Peatland Carbon Network website (https://peatlands.lehigh.edu). This database will be useful in future studies of ecosystem – C cycle – climate interactions and for modeling long-term peatland dynamics.

In the following sub-sections, we present the criteria for site selection and the protocols used to develop the database. In an effort to only analyze and synthesize *peat* samples, inorganic-rich horizons often found at the base of the peat cores were removed from the database. When available, stratigraphic information was used to distinguish peat versus non-peat material. For example, gyttja (organic-rich lake sediments) was excluded from the dataset, as well as marshy, clayey, and silty sediments. When stratigraphic information was not available, a BD value of 0.5 g/cm³ was used as a cutoff between peat and non-peat material. This value was chosen on the basis of stratigraphic information from peatland records where peaty sediments with BD values up to 0.5 g/cm³ were identified. We acknowledge that this cutoff value is arbitrary, and that our dataset likely contains some non-peat samples. Inorganic horizons (e.g. tephra layers) were also excluded from the database.

Peat properties

A total of 232 peat cores (181 sites) were used for characterizing peat properties, although not all cores have all types of peat properties available (Figure 2a). This dataset contains 139 cores from Eurasia (including 109 cores from Russia) and 93 cores from North America (Figure 1). While approximately half of these cores were sampled and analyzed at high resolution (1–5 cm increments), the remainder was sampled at lower resolution, typically at 10 cm increments. Dry BD (g/cm³), OM content (OM%; gravimetric %), and elemental C and N concentration
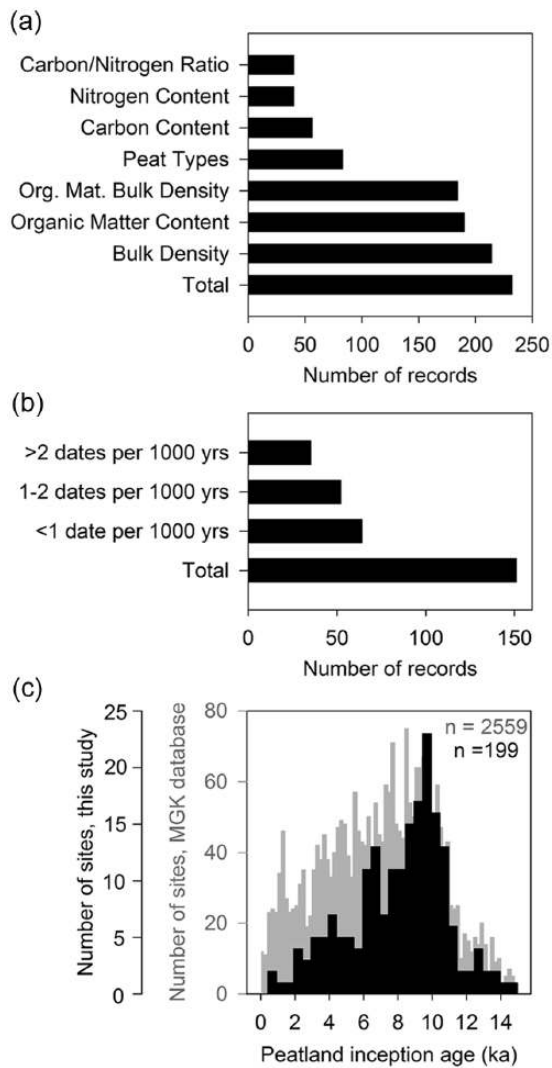
Figure 2. Overview of data availability. (a) Number of cores (total = 238) containing information on carbon/nitrogen ratio (*n* = 40), nitrogen content (*n* = 40), carbon content (*n* = 56), peat types (*n* = 83), organic matter bulk density (*n* = 184), organic matter content (*n* = 190), and bulk density (*n* = 214). (b) Number of cores (total = 151) with a dating quality better than two dates per 1000 years (*n* = 35), one to two dates per 1000 years (*n* = 52), and less than one date per 1000 years (*n* = 64). (c) Number of calibrated basal peat ages (median) in 500-year bins from the database (*n* = 199) compared with all northern hemisphere basal peat ages (median) in 200-year bins (*n* = 2559, MGK data from Gorham et al., 2007; Korhola et al., 2010; MacDonald et al., 2006).

values were compiled and synthesized. On the basis of these raw datasets, C/N mass ratio and OMBD (g OM/cm³) were calculated. These peat geochemical values are examined in light of peat stratigraphy, peat ages, and geographic regions. The following paragraphs briefly describe the protocols used to obtain these values.

Peat stratigraphic information was obtained for 83 peat cores ('peat types' in Figure 2a) for which plant macrofossil analysis or detailed peat description had been performed following standard techniques (e.g. Mauquoy and Van Geel, 2007; Troels-Smith, 1955). This peat stratigraphic information was condensed into the following five peat types: *Sphagnum*, herbaceous, woody, brown moss, and humified peat. The uncertainty associated with classifying peat samples mostly relates to the uniformity of naming convention used among the investigators. For example, a peat sample that contains sizable fractions of brown moss and humified peat may be classified by an investigator as 'brown moss peat' and by

another one as 'humified peat'. We recognize that, because of their nature, brown moss and humified peat types might be less uniform than *Sphagnum* or herbaceous peat types. We included as much stratigraphic information as possible in the database, though ambiguous or imprecise descriptions were left out to avoid further confusions.

Dry BD and OM content were determined following standard procedures (Chambers et al., 2011; Dean, 1974). Peat samples of a known fresh volume were either freeze-dried or oven-dried at *c.* 100°C until constant weight was reached and weighed to determine BD, then burned at 500–600°C for 1–4 h and weighed again to determine OM content. The accuracy of these measurements mostly depends on sample handling (care must be taken to prevent peat compaction in the field and in the laboratory) and the analytical error associated with weighing. The product of BD (g/cm³) and OM content (OM%) of each peat sample was used to calculate OMBD (g OM/cm³), also referred to as ash-free bulk density (AFBD) or organic bulk density (OBD) in the literature (Björck and Clemmensen, 2004; Yu et al., 2003). We compiled a total of 21,220 BD measurements, 18,973 OM content values, and computed 18,544 OMBD values (Table 1).

Total peat C and N content was directly measured by combustion and elemental analysis of dry peat samples (Chambers et al., 2011). We compiled 3741 C and 3365 N measurements (Table 1). We also computed a total of 3362 C/N mass ratio values.

Finally, the regression between peat C content (C%) and peat OM content (OM%) for each peat type is presented as an estimate for C content in OM (OC%). A total of 995 samples were used in this analysis. The slope of each one of these regressions is interpreted as the 'conversion factor' from OM% to OC%, such that it provides an indirect way for estimating the C% content of ash-free peat for investigators who do not perform elemental C measurements directly.

Peat-core chronology

Peat-core chronologies were almost exclusively based on radiocarbon (^{14}C) dates that were determined mostly by accelerator mass spectrometry (AMS) on terrestrial plant macrofossils or bulk peat (Piotrowska et al., 2011). A few older chronologies were based on conventional ^{14}C dating of bulk samples. Because no systematic offset has been observed in the ^{14}C age of bulk versus non-woody plant macrofossils (GM MacDonald, 2013, personal communication), the use of bulk dates is justifiable. For the purpose of this study, all ^{14}C dates were calibrated to calendar years before present (cal. yr BP) using the program CALIB 6.1.0 (Stuiver and Reimer, 1993) with the IntCal09 calibration dataset (Reimer et al., 2009). In this paper, ages are reported in thousands of calibrated years before present (kyr).

Age–depth relationships were established for all continuous peat cores for which at least five age determinations were available (*n* = 151 cores). Except for a few palynostratigraphic and tephrochronologic markers, nearly all records have chronologies exclusively based on ^{14}C ages (Supplementary Table S1, available online). Chronologies were obtained through linear interpolation of calibrated ages between dated horizons. Single-age estimates were taken from the mid-point of each calibrated 2σ probability distribution. This parsimonious approach captures general patterns of temporal changes in peat accumulation and allows for analysis of peat C accumulation trajectories (e.g. Telford et al., 2004). Although more sophisticated approaches are possible (e.g. Charman et al., 2013), we seek to make the fewest or simplest assumptions for this analysis because the temporal resolution target for peat C accumulation rate calculations is relatively low (at 500 years). In the cases where the original investigator identified hiatuses (e.g. peat loss caused by erosion or fire) or depositional anomalies (e.g. thick tephra layers that interrupted peat accumulation) along their peat records, these gaps were taken into consideration when building
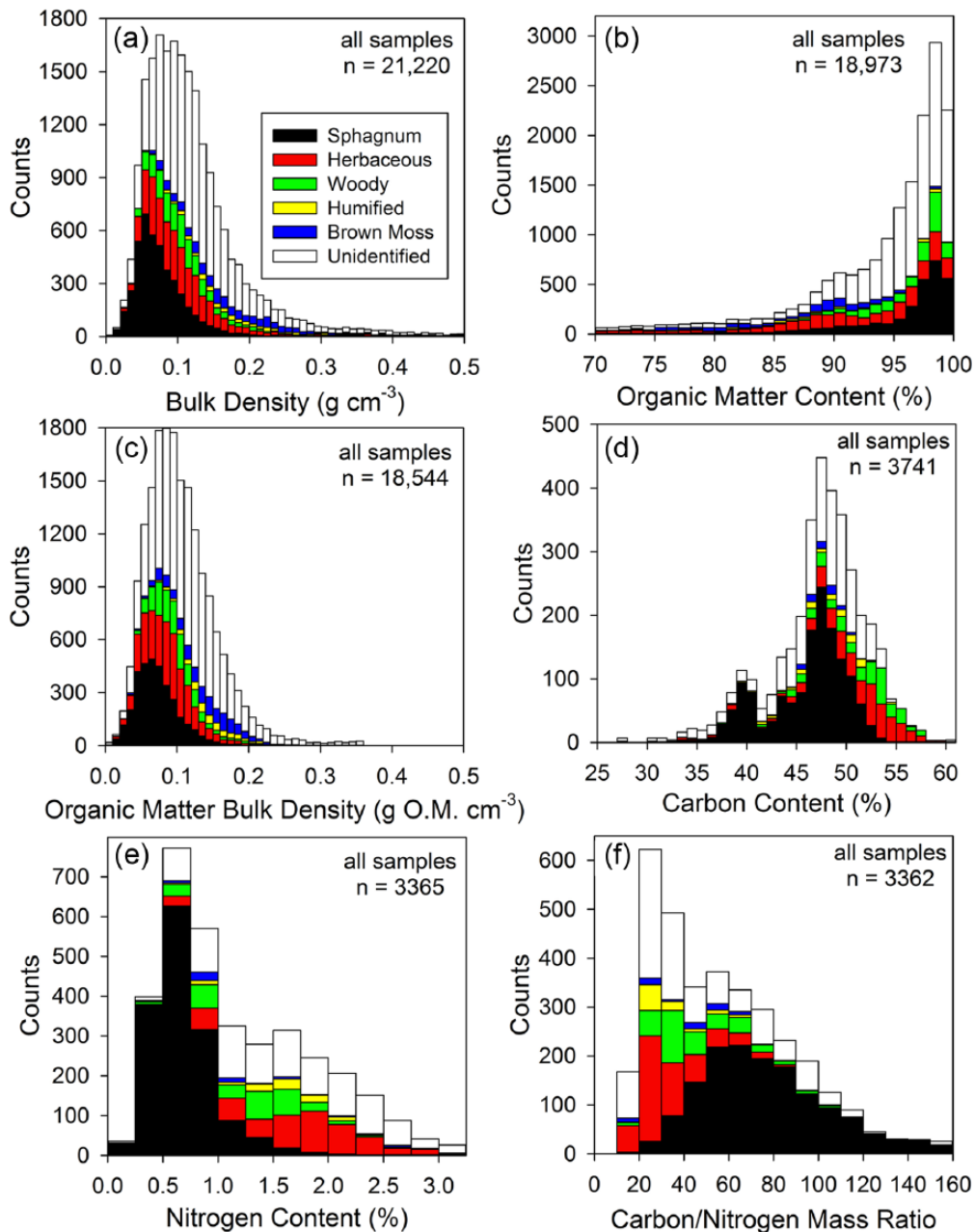
Figure 3. Distribution histograms of peat properties in northern peatlands: (a) frequency distribution of bulk density for unidentified peat type samples (white bars) and different peat types (color bars), (b) frequency distribution of organic matter content for different peat types, (c) frequency distribution of organic matter bulk density for different peat types, (d) frequency distribution of carbon content for different peat types, (e) frequency distribution of nitrogen content for different peat types, and (f) frequency distribution of carbon/nitrogen mass ratio for different peat types.

age–depth relationships (Glaser et al., 2012). Otherwise, peat records were assumed to be continuous.

In an effort to assess the representativeness of our samples in terms of peatland inception timing, peat basal ages were compiled and compared with results from large datasets (Gorham et al., 2007; Korhola et al., 2010; MacDonald et al., 2006). Peat inception ages from 199 sites (Supplementary Table S1, available online) were summed and binned in 500-year intervals.

Long-term rates of carbon and nitrogen accumulation

A total of 151 peat cores from 127 sites were used for estimating rates of peat C accumulation. This dataset contains 96 cores from 78 North American sites and 55 cores from 49 Eurasian sites (Figure 1). Of the 33 sites presented in Yu et al.'s (2009) study, 25 were used in this study (Supplementary Table S1, available online). The remaining 8 sites did not fulfill our dating

quality criterion (presented below). The dating quality of each record was determined by the quotient of the calibrated peat basal age and the number of age determinations. For example, a 10,000-year-old peat core with a chronology constrained by 10 ^{14}C dates was attributed a dating quality of one date per 1000 years. About 58% of our 151 cores were characterized by an acceptable dating quality of one to two ^{14}C dates per 1000 years (Figure 2b). These resolutions are well suited to capture millennial-scale variations in C accumulation. Several peat cores with more than two ^{14}C dates per 1000 years (*n* = 35 cores) were available from North America and Europe. The lower dating quality cores (<1 date per 1000 years) were unevenly distributed and comprise 44% of the North American records and 40% of the Eurasian records.

The long-term rate of peat C accumulation was calculated for each core following one of the following five approaches (Supplementary Table S1, available online): (1) whenever possible,

Table 1. Peat properties in northern peatlands. Means and standard deviations are presented, along with the number of samples (n).

	Sphagnum	Herbaceous	Woody	Humified	Brown Moss	Overall[a]
Bulk density (g/cm³)	0.076 ± 0.038 (n = 4372)	0.118 ± 0.075 (3188)	0.108 ± 0.047 (1584)	0.192 ± 0.082 (452)	0.177 ± 0.076 (1114)	0.118 ± 0.069 (21,220)
Organic matter content (%)	94.3 ± 9.3 (3297)	85.6 ± 15.4 (3121)	92.0 ± 13.5 (1587)	78.4 ± 17.8 (418)	81.4 ± 15.5 (1090)	90.7 ± 13.0 (18,973)
Organic matter bulk density (g OM/cm³)	0.073 ± 0.031 (3332)	0.089 ± 0.036 (2854)	0.098 ± 0.032 (1388)	0.144 ± 0.036 (418)	0.136 ± 0.043 (1090)	0.105 ± 0.051 (18,544)
Carbon content in total peat (%)	46.0 ± 4.1 (1520)	50.5 ± 4.9 (519)	50.9 ± 4.0 (308)	47.4 ± 4.1 (96)	47.9 ± 2.8 (72)	46.8 ± 6.1 (3741)
Carbon content in organic matter (%)	42.3 ± 3.0[b] (454)	51.1 ± 1.7[b] (147)	51.4 ± 3.4[b] (59)	53.2 ± 2.6[b] (58)	50.0 ± 2.0[b] (44)	49.2 ± 2.4[c] (458)
Nitrogen content in peat (%)	0.7 ± 0.3 (1523)	1.7 ± 0.6 (518)	1.3 ± 0.5 (308)	1.5 ± 0.4 (96)	1.4 ± 0.7 (60)	1.2 ± 0.7 (3365)
Carbon/nitrogen mass ratio	81.0 ± 49.2 (1520)	34.4 ± 15.0 (518)	45.3 ± 19.1 (308)	36.0 ± 17.6 (96)	42.9 ± 18.8 (60)	55 ± 33 (3362)

[a]Includes samples for which peat type was not ascribed.
[b]Obtained from regression between carbon content and organic matter content (see 'Database and analysis' section).
[c]Includes all herbaceous, woody, humified, and brown moss samples, as well as *Sphagnum* samples older than 0.5 kyr (see 'Results' section).

Table 2. Northern peatland peat properties by regions. Means and standard deviations are presented, along with the number of samples in parentheses (n).

	Alaska	Western Canada	Hudson Bay and James Bay	Eastern Canada/ United States	Western European Islands	Continental Europe	Fennoscandia	Western Russia	Eastern Russia and Asia
Bulk density (g/cm³)	0.168 ± 0.087 (n = 1659)	0.166 ± 0.076 (3635)	0.097 ± 0.038 (6002)	0.100 ± 0.039 (2834)	0.055 ± 0.027 (656)	0.120 ± 0.139 (410)	0.075 ± 0.043 (562)	0.118 ± 0.070 (2701)	0.116 ± 0.063 (2761)
Organic matter content (%)	76.6 ± 18.8 (1659)	91.6 ± 8.1 (3442)	94.8 ± 8.2 (5129)	97.8 ± 6.5 (1835)	97.5 ± 1.8 (227)	97.4 ± 5.43 (305)	95.6 ± 8.7 (789)	94.6 ± 10.3 (2666)	80.3 ± 16.7 (2700)
Organic matter bulk density (g OM/cm³)	0.119 ± 0.049 (1659)	0.151 ± 0.062 (3441)	0.088 ± 0.029 (5129)	0.107 ± 0.028 (1750)	0.055 ± 0.035 (227)	0.056 ± 0.028 (222)	0.073 ± 0.034 (422)	0.106 ± 0.058 (2773)	0.088 ± 0.034 (2700)
Carbon content in total peat (%)	42.4 ± 3.7 (64)	45.0 ± 4.3 (382)	47.9 ± 4.5 (1026)	48.9 ± 3.7 (1084)	54.0 ± 2.5 (242)	38.9 ± 1.3 (60)	44.4 ± 5.7 (580)	49.2 ± 3.2 (74)	36.0 ± 9.2 (229)
Nitrogen content in total peat (%)	1.3 ± 0.6 (64)	1.1 ± 0.8 (265)	1.6 ± 0.7 (910)	0.9 ± 0.5 (1084)	1.6 ± 0.4 (242)	0.7 ± 0.1 (60)	1.0 ± 0.5 (565)	1.6 ± 0.9 (44)	1.4 ± 0.6 (131)
Carbon/nitrogen mass ratio	43.9 ± 32.8 (64)	62.4 ± 37.5 (265)	39.5 ± 23.7 (910)	77.2 ± 56.1 (1084)	35.7 ± 10.8 (242)	54.2 ± 7.6 (60)	57.9 ± 31.4 (562)	40.8 ± 21.7 (44)	34.2 ± 21.9 (131)

peat-core chronology was combined with BD and C% for each depth increment (n = 47 cores); (2) in the cases where direct C measurements were lacking, peat-core chronology was combined with OMBD measurements and a mean organic C value of 49% in OM (n = 57 cores); (3) for cores that lacked OMBD and direct C%, peat-core chronology was combined with BD measurements and a mean C content of 47% in total peat (n = 3 cores); (4) whenever neither BD nor C% was directly available from the cores, long-term rate of peat C accumulation was calculated for each core by combining time-dependent bulk densities (0.08 g/cm³ at 0–0.5 kyr, 0.12 g/cm³ at 0.5–6 kyr, 0.14 g/cm³ at 6–12 kyr) with a mean C content of 47% in total peat for each dated interval (n = 32 cores); and (5) peat C accumulation rates for the remaining 12 cores were directly obtained from published figures and tables. For all the cores, time-weighted peat C accumulation rates were summed and binned in 500-year intervals. It is important to note that such reconstructions are 'apparent rates' that are different from true rates of C accumulation in peatlands because decomposition processes have been affecting old peat layers for thousands of years (Turunen et al., 2002). Finally, the long-term rate of peat N accumulation was calculated by combining our binned peat C accumulation rates with time-dependent C/N values (65 at 0–6 kyr and 40 at 6–10 kyr).

Results

Peat properties

Descriptive statistics of dataset. The frequency distribution of each peat property is shown in Figure 3. Mean values and standard deviations (SDs) for all peat properties are presented by peat type in Table 1, and by region in Table 2.

BD values (n = 21,220) range from 0.003 to 0.498 g/cm³, with a mean value of 0.118 ± 0.069 g/cm³ (1 SD). A one-way analysis of variance (ANOVA) reveals an effect of peat type on BD ($F(10,709)$ = 941, p < 0.0001), with all peat types significantly different from each other on the basis of post hoc Tukey's LSD tests (p < 0.0001). In increasing order, mean BD of the peat types is *Sphagnum* < Woody < Herbaceous < Brown Moss < Humified (Table 1).

OM content (n = 18,973) has a mean value of 90.7 ± 13% (1 SD) and a median of 95.7%. The ANOVA reveals an effect of peat type on OM content ($F(9512)$ = 349, p < 0.0001), with all peat types significantly different from each other (Tukey's LSD: p < 0.0001). In decreasing order, mean OM content of the peat types is *Sphagnum* > Woody > Herbaceous > Brown Moss > Humified (Table 1).

OMBD (n = 18,544) ranges from 0.003 to 0.452 g OM/cm³, with a mean value of 0.105 ± 0.051 g OM/cm³ (1 SD). The ANOVA reveals an effect of peat type on OM density ($F(9081)$ = 942, p < 0.0001), with all peat types significantly different from each other (Tukey's LSD: p < 0.0001). In increasing order, mean OM density of the peat types is *Sphagnum* < Herbaceous < Woody < Brown Moss < Humified (Table 1).

C content in total peat (n = 3741) ranges from 30% to 60%, with a mean value of 46.8 ± 6.1% (1 SD) and a median of 47.8%. While the lowest values (<35%) are almost exclusively associated with samples from Alaska, western Canada, Fennoscandia, and eastern Russia, the highest values (>55%) are characteristic of sites located in the western European Islands and Fennoscandia. The ANOVA reveals an effect of peat type on C% ($F(2494)$ = 161, p < 0.0001), with *Sphagnum* samples significantly different from other peat types (Tukey's LSD: p < 0.0001). Herbaceous and woody peats are distinct from other types, but indistinguishable from one another (Tukey's LSD: p = 0.238). Likewise, humified and brown moss peats are distinct from other types, but indistinguishable from each other (Tukey's LSD: p = 0.448). In increasing order, mean C% of the peat types is *Sphagnum* < Humified = Brown Moss < Herbaceous = Woody (Table 1). The frequency distribution of C% in peat is also characterized by a second, though minor, mode at 40% (Figure 3d). The latter is mostly associated with *Sphagnum* peat samples, as their average C% is significantly lower than those for other peat types (Table 1). This difference is likely caused by the high content of complex and recalcitrant compounds found in *Sphagnum* tissues such as lipids and waxes, which have lower C% than more labile biopolymers such as cellulose (Cagnon et al., 2009).

On the basis of 995 samples for which both OM% and C% were quantified, we developed conversion factors (slopes of linear regressions) for several peat types to estimate OC% (Figure 4). There is a noticeable difference between the slope of *Sphagnum* peat (0.423 ± 0.030; n = 454) and that of non-*Sphagnum* peat (0.514 ± 0.024; n = 308). The C content in OM (OC%) for *Sphagnum* peat is smaller than expected at 42.3 ± 3.0% (e.g. Bauer et al., 2006; Beilman et al., 2009; Table 3). As the majority of our *Sphagnum* samples for this specific analysis are younger than 0.5 kyr (304 out of 454 samples) and extracted from raised bogs, it is very likely that our estimated OC% biases toward young and less decomposed *Sphagnum*. This 'young *Sphagnum* peat effect' heavily influenced the slope of the overall relation between C% and OM% (0.467 ± 0.045) because of the overrepresentation of *Sphagnum* samples in the dataset (454 out of 995 samples). To minimize this bias when estimating mean OC% in peat, all 304 young *Sphagnum* samples were removed from the dataset, yielding an overall conversion factor of 0.492 ± 0.024.

N content in peat (n = 3365) ranges from 0.04% to 3.39%, with a mean value of 1.2 ± 0.7% (1 SD). The frequency distribution is asymmetric and characterized by a mode at 0.65% (Figure 3e). The latter is largely because of the overrepresentation of *Sphagnum* peat samples (having low N content) in our database. The ANOVA reveals an effect of peat type on N content ($F(2504)$ = 666, p < 0.0001), with *Sphagnum* and herbaceous peat types significantly different from each other and from all other types (Tukey's LSD: p < 0.0001). Humified and brown moss peats are distinct from other types, but indistinguishable from each other (Tukey's LSD: p = 0.113). Likewise, woody and brown moss peats are indistinguishable from one another (Tukey's LSD: p = 0.240). In increasing order, mean N% of the peat types is *Sphagnum* < Woody = Brown Moss = Humified < Herbaceous (Table 1).

C/N mass ratio (n = 3362) ranges from 12 to 217, with a mean value of 55 ± 33 (1 SD). The frequency distribution is asymmetric and characterized by a mode at 25 (Figure 3f). While the distribution mode (25) is associated with non-*Sphagnum* peat types, the distribution mean (55) is skewed toward *Sphagnum* peat samples owing to their overrepresentation in our database (Figures 3f). The ANOVA reveals an effect of peat type on C/N ratio ($F(2501)$ = 174, p < 0.0001), with *Sphagnum* peat significantly different from all other types (Tukey's LSD: p <0.0001). Woody peat is distinguishable from all peat types except for brown moss peat (Tukey's LSD: p = 0.665). Herbaceous and humified peat types are indistinguishable from one another (Tukey's LSD: p = 0.721). In decreasing order, the mean C/N ratio of peat types is *Sphagnum* > Woody = Brown Moss > Humified = Herbaceous (Table 1).

Temporal changes in peat properties. We find a decreasing trend in BD over the Holocene (Figure 5a), with the densest peat characterizing the oldest samples (8–10 kyr) and the least dense peat characterizing the youngest samples (0–2 kyr). This trend is most likely attributable to the progressive decomposition and subsequent compaction of peat over time, as well as to higher ash content in early-stage peat (likely from fens). Conversely, a clear increasing trend in OM content (OM%) is found over the
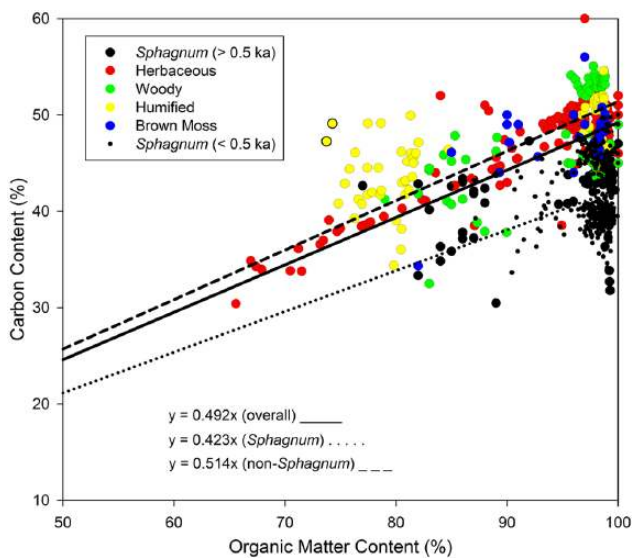
Figure 4. Relation between carbon content and organic matter content in northern peatlands. The slope of each regression line is used as a conversion factor for estimating carbon content from organic matter content.

Holocene (Figure 5b), with the greatest OM% characterizing the youngest samples (0–2 kyr) and the least OM% characterizing the oldest samples (8–10 kyr). This trend is most likely attributable to higher inorganic material inputs during early-stage peatland development as well as to a greater loss of OM in the deeper portions of peat profiles. OMBD remains relatively constant over the Holocene (Figure 5c) because of the opposite trends exhibited by BD and OM% (Figure 5a and b). The only exceptions are the low OMBD values characterizing the youngest samples (<0.5 kyr), probably because of the large proportion of young, undecomposed *Sphagnum* peat samples.

C content in peat remains uniform over the Holocene (Figure 5d), except for slightly lower C% during the late Holocene. We find a decreasing trend in N% over the Holocene, such that young peat deposits are associated with low N% (Figure 5e). Peat deposits older than 6 kyr are mostly associated with low C/N ratios, whereas peat samples younger than 6 kyr are characterized by high C/N values (Figure 5f).

In general, *Sphagnum* peat is characterized by lower BD, OMBD, C%, N%, and C/N ratio than samples composed of non-*Sphagnum* peat (Figure 6). Therefore, peatland development could explain much of the aforementioned temporal trends (Figure 5), as early-stage rich fens are typically characterized by non-*Sphagnum* peat, whereas late-stage poor fens and bogs are *Sphagnum*-dominated (Figure 6h).

Spatial differences in peat properties. Significant differences in BD are found at the regional scale (Table 2). The densest peat is observed in Alaska (mean = 0.168 ± 0.087 g/cm³) and western Canada (mean = 0.166 ± 0.076 g/cm³), whereas the least dense peat is found from the western European Islands (mean = 0.055 ± 0.027 g/cm³). OMBD values follow a similar pattern across these regions (Table 2). These differences are strongly correlated with peat types and sample ages, with the Alaskan and western Canadian samples largely constituted of herbaceous, humified, and brown moss peat types. OM% does not vary much between regions (>90% in all regions), with the notable exception of Alaskan and eastern Russian/Asian peatlands that exhibit mean values of 76.6 ± 18.8% and 80.3 ± 16.7%, respectively (Table 2). Eolian dust and tephra ash inputs to some peatlands in Alaska, Kamchatka, and Japan might partly explain such low OM% values.

Peat inception ages and long-term rates of carbon and nitrogen accumulation

Calibrated ages (mid-point) for peat inception range from 0.6 to 15 kyr, and the frequency distribution is characterized by a mode at 11–9 kyr (Figure 2c). The latter corresponds with peat inception peaks in the West Siberian Lowlands and in Alaska. In general, our samples are in agreement with much larger networks of peat basal ages (Gorham et al., 2007; Korhola et al., 2010; MacDonald et al., 2006; Ruppel et al., 2013; Smith et al., 2004; Yu et al., 2013).

The time-weighted long-term rate of C accumulation averages 22.9 ± 2.0 g C/m²/yr (standard error of mean (SEM); Figure 7b). Values exhibit an increasing trend that initially peaks during the early Holocene between 10 and 7.5 kyr at 27.0 ± 2.6 g C/m²/yr. This peak is largely caused by rapid peat accumulation in Alaska, the Western Siberia Lowlands, and southeastern Canada. The remainder of the Holocene is characterized by a decreasing trend in C accumulation rates from 24 to 18 g C/m²/yr and a time-weighted mean at 22.0 ± 1.9 g C/m²/yr (Figure 7b). There is a notable minimum value between 3 and 1.5 kyr at 18–19 g C/m²/yr. Lack of decomposition probably explains most of the apparent increase in accumulation over the past millennium (24–32 g C/m²/yr), as young peat appears to be accumulating more quickly than old peat simply because the former has undergone less decomposition than the latter (Clymo, 1984).

The time-weighted long-term rate of N accumulation averages 0.5 ± 0.04 g N/m²/yr (SEM; Figure 7c). While the mid- and late Holocene (6–0 kyr) are characterized by the lowest rates of N accumulation at 0.34 g N/m²/yr, the highest rates (0.61 g N/m²/yr) occur between 12 and 6 kyr (Figure 7c). This trend mirrors that of C accumulation (Figure 7b), as C and N sequestration rates are both mainly influenced by peat density and peat accumulation rate. The low rates of N accumulation over the past 6 kyr might also relate to the increasing presence and persistence of *Sphagnum* (having high C/N ratio and low N concentration) in northern peatlands (Figures 6 and 7).

Discussion

### Representativeness of the database for northern peatlands

The present database contains the most comprehensive compilation of peat properties and C accumulation records for northern peatlands. The previous large-scale synthesis (Yu et al., 2009) only contained 33 sites and lacked records from the Hudson Bay lowlands and the Russian Far East, and had limited sites from West Siberia and the western European Islands. The present database fills gaps from these regions.

However, European Russia, East Siberia, and the Russian Far East clearly remain poorly studied regions in terms of northern peat C stocks and accumulation histories (Figure 1). A wetland map by Stolbovoi and McCallum (2002) suggests that shallow peaty deposits (<50 cm) interspersed with few deeper peat bogs (>50 cm) dominate the Far East Russian landscape. Most of these deeper peatlands are presumably found in Kamchatka and Sakhalin (Stolbovoi, 2002). This broad portrait is, however, based on fewer than 30 soil profiles from across East Siberia and Far East Russia (Stolbovoi et al., 2001), making it difficult to evaluate the importance of this region in the northern peatland C cycle. In general, peat C stocks in Eastern Russia may not be as massive as those from West Siberia or European Russia (Stolbovoi and McCallum, 2002). Therefore, understanding how these shallow peatlands in East Siberia and the Russian Far East have developed during the Holocene would provide useful end-members of climate controls of peat C accumulation, but these peatlands do not seem to represent a large missing C stock.

Table 3. Comparison of northern peatland peat properties estimates with other published values. Means and standard deviations are presented, along with the number of samples (*n*) when available.

Bulk density (g/cm³)	Organic matter content (%)	Organic matter bulk density (g OM/cm³)	Carbon content in organic matter (%)	Carbon/nitrogen mass ratio	Region	Reference
–	–	0.094 open fens and bogs 0.105 wooded and shrubby fens	51.8 ± 4.7 (n = 253)	–	Western Canada	Vitt et al. (2000)
0.073 ± 0.029 Sphagnum 0.091 ± 0.025 brown moss 0.110 ± 0.037 sedge moss 0.211 ± 0.061 humified 0.138 ± 0.036 wood	95.5 ± 2.6 Sphagnum 90.3 ± 6.6 brown moss 91.4 ± 4.4 sedge moss 73.6 ± 13.0 humified 87.8 ± 6.3 wood	0.069 ± 0.028 Sphagnum 0.082 ± 0.023 brown moss 0.100 ± 0.032 sedge moss 0.149 ± 0.023 humified 0.120 ± 0.029 wood	50.7 ± 5.0 Sphagnum 51.9 ± 3.4 brown moss 53.4 ± 2.9 sedge moss 54.0 ± 3.8 humified 52.1 ± 3.5 wood	–	Western Canada	Bauer et al. (2006)
–	–	0.0784 bogs	52.8 (n = 276)	–	Eastern Canada and United States	Gorham (1990)
–	–	0.112	51.7	–	Eastern Canada and United States	Gorham (1991)
0.128 ± 0.065	96.26 ± 3.16	0.123[a]	52	–	West Siberia Lowlands	Sheng et al. (2004)
–	–	–	51 ± 5 Sphagnum[b] 55 ± 3 non-Sphagnum[b] 52 ± 3 overall[b]	–	West Siberia Lowlands	Beilman et al. (2009)
–	–	0.074 bogs 0.081 fens	50	–	Finland	Turunen et al. (2002)
0.118 ± 0.069 (n = 21,220)	90.7 ± 13.0 (n = 18,973)	0.105 ± 0.051 (n = 18,544)	49.2 ± 2.4 (n = 458)	55 ± 33 (n = 3362)	Circum-Arctic	This study

[a]This value was obtained by multiplying bulk density (0.128 g/cm³) by organic matter content (96.26%).
[b]Standard errors.
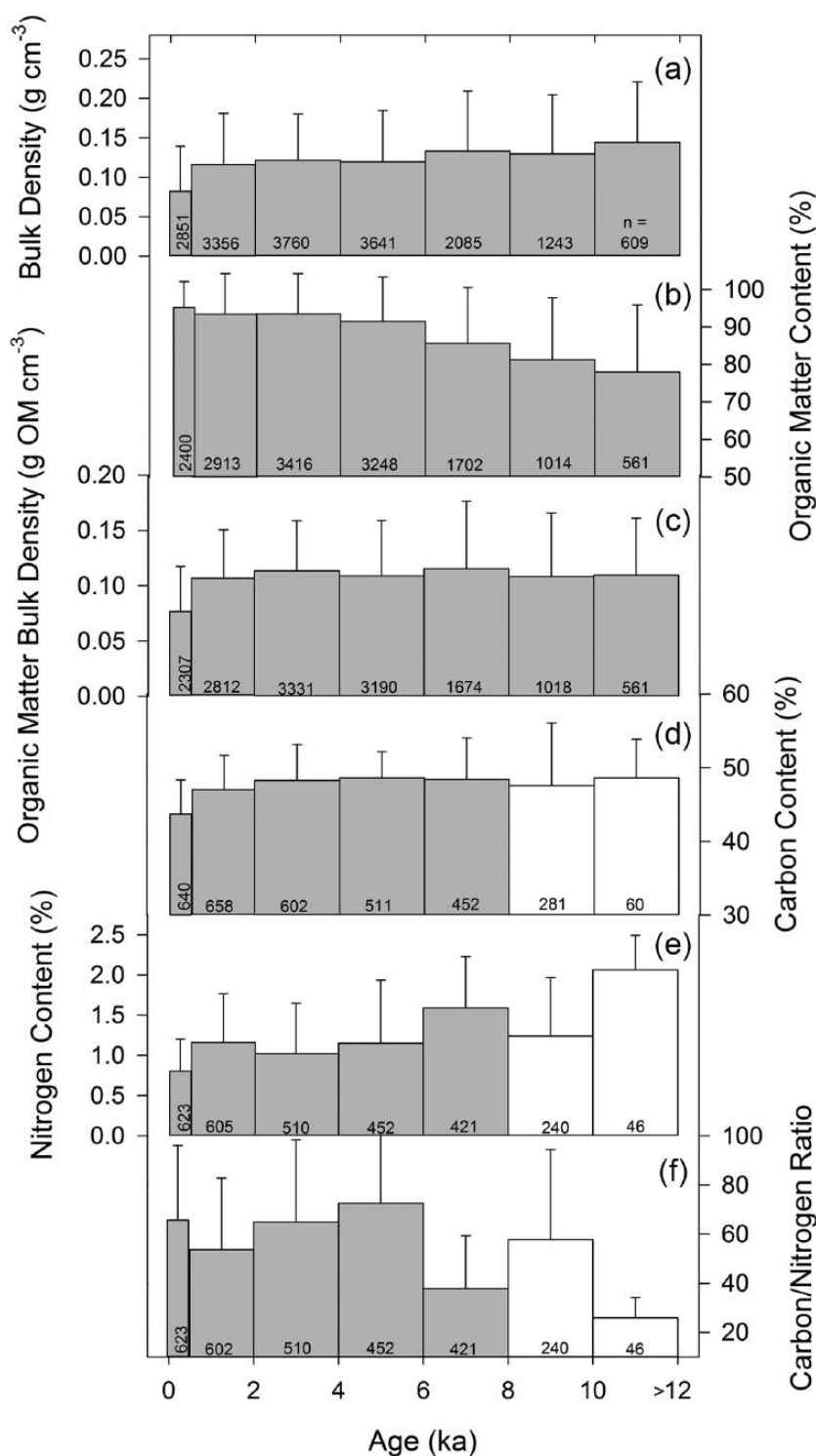
Figure 5. Temporal patterns of peat properties (mean, standard deviation, and number of samples): (a) bulk density, (b) organic matter content, (c) organic matter bulk density, (d) carbon content, (e) nitrogen content, and (f) carbon/nitrogen mass ratio. White bars represent values that were based on a limited number of samples and peat records.

Northern peatland soil properties: key findings and uncertainties

Peat-carbon stocks. Several studies have quantified the soil C density and total C pool of peatlands using different approaches (e.g. Armentano and Menges, 1986; Gorham, 1991; Yu et al., 2010). These methods have led to total C pool estimates for northern peatlands that vary by at least a factor of two, from 234 to 547 GtC (Lappalainen, 1996; Yu et al., 2010; see Yu (2012) for a review). Many of these studies have combined mean peat depth, modern peatland area, and a single mean C density value (BD × C% or

OMBD × OC%) in their calculations (e.g. Gorham, 1991). Applying Gorham's (1991) mean peat depth and peatland area estimates to the mean BD and C% results from our database yields a C pool estimate of 436 GtC (2.3 m × 3.42 Mkm² × 0.118 g /cm³ × 47% C). However, it is well documented that most peatlands undergo a shift from herbaceous to *Sphagnum* peat during their developmental history (Hughes, 2000; Figure 6h) and that different BD, C%, and rates of peat accumulation are associated with fen and bog peats (e.g. Vitt et al., 2000; Figure 6). We also know that peat C accumulation rates have varied asynchronously between regions throughout the Holocene as a result of regional changes in
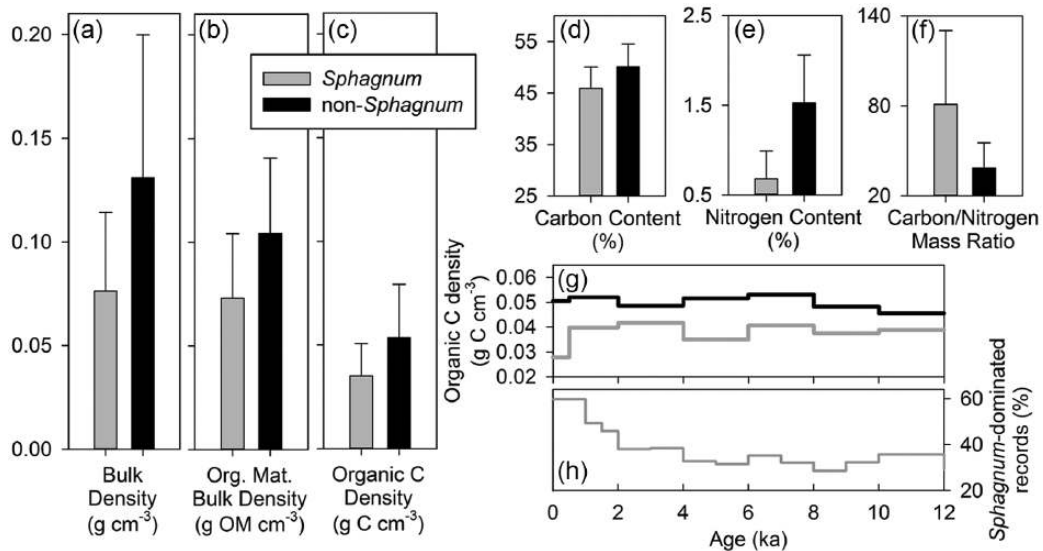
Figure 6. Main differences between *Sphagnum* and non-*Sphagnum* peat samples: (a) bulk density, (b) organic matter bulk density, (c) organic carbon bulk density, (d) carbon content, (e) nitrogen content, (f) carbon/nitrogen mass ratio, (g) temporal pattern of organic carbon bulk density, and (h) proportional change in the number of peat records that are *Sphagnum*-dominated, presented as a percentage of the total number of records.
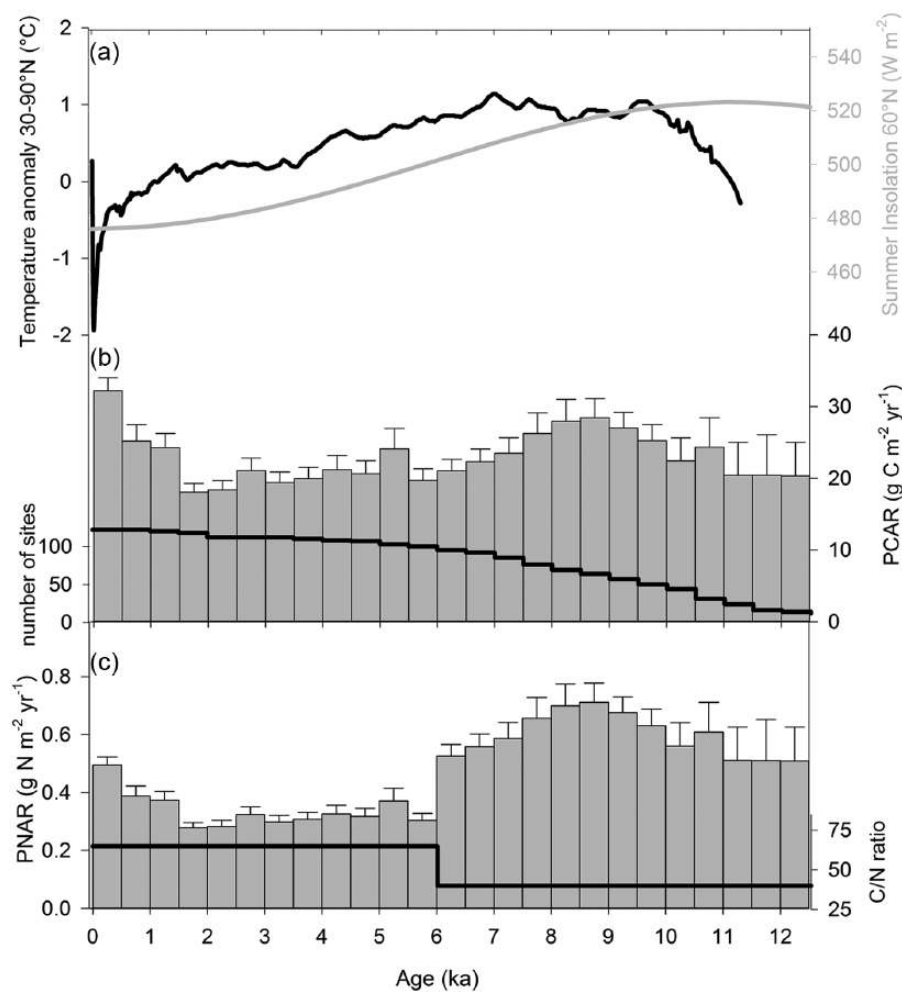
Figure 7. Long-term apparent rate of carbon and nitrogen accumulation from northern peatlands (*n* = 127 sites). (a) Summer insolation at 60°N (data from Berger and Loutre, 1991) and temperature anomaly from an 11,300-year reconstruction for the northern region from 30° to 90°N (data from Marcott et al., 2013). Temperature anomaly was calculated based on the 1961–1990 temperature averages. (b) Mean peat carbon accumulation rates (PCAR) and standard error in 500-year bins. The number of sites per 500-year bins is also presented as step lines. (c) Mean peat nitrogen accumulation rates (PNAR) and standard error in 500-year bins. These values were obtained using different C/N values over time, as indicated by the line.

hydroclimatic conditions (e.g. Charman et al., 2013; Yu et al., 2009). Therefore, we argue that reconstructing Holocene changes in peat C accumulation on the basis of *measured* peat C density and reliable peat-core chronologies constitutes a step forward in providing the best possible peat C stock estimates (see, for example, Yu et al., 2010). It also allows for quantifying spatial and temporal differences in rates of peat C accumulation, as well as the temporal trajectories of peat C fluxes to the atmosphere (MacDonald et al., 2006; Yu et al., 2013). However, better maps of the present peatland area (and its change over time) are still needed to improve current peat C stock estimates.

Carbon content in OM. For each peat layer, peat C density can be estimated by the product of either (1) BD and C content in total peat (BD × C%) or (2) AFBD and C content in OM (OMBD × OC%). It could be argued that the first option is preferable when estimating peat C stocks, as it produces values that are directly comparable with routine soil C measurements from other terrestrial ecosystems. However, the present database clearly indicates that the majority of peatland scientists routinely analyze OM content (OM%; $n = 18,973$ samples) rather than C% ($n = 3741$ samples) along peat cores. To provide a way to estimate OC% from OM%, we developed the following conversion factors: 42.3 ± 3.0% for *Sphagnum* peat, 51.4 ± 2.4% for non-*Sphagnum* peat, and 49.2 ± 2.4% overall (Figure 4 and Table 1).

While the overall peat and the non-*Sphagnum* peat conversion factors are in line with those from previous studies (e.g. Beilman et al., 2009; Gorham, 1991; Turunen et al., 2002; Vitt et al., 2000), the *Sphagnum* peat factor is lower than other estimates (e.g. Bauer et al., 2006; Beilman et al., 2009; Table 3). Indeed, our mean OC% *Sphagnum* value at 42.3% is close to that of surface *Sphagnum* tissues, suggesting that it constitutes a valid estimate for ash-free and poorly decomposed *Sphagnum* peat. As previously mentioned, this bias toward low OC% is because of a large number of *Sphagnum* samples younger than 0.5 kyr (304 out of 454 *Sphagnum* samples).

Although each one of the three conversion factor slopes was significant ($p < 0.0001$), there is a noticeable scatter in the data (Figure 4) that cannot solely be explained by the ~1% analytical error associated with the loss-on-ignition procedure (Heiri et al., 2001). The progressive accumulation of recalcitrant C in old samples (lignin ~60% C vs cellulose ~42% C), assuming it occurs at a greater rate than the loss of OM in the deeper portions of peat profiles, could explain why C% appears higher than our OC% conversion factors (Cagnon et al., 2009). The presence of inorganic C, particularly for the humified and brown moss peat types, could also explain these results.

Oligotrophication and the fen-to-bog transition in northern peatlands. *Sphagnum* and non-*Sphagnum* peat types were characterized by very different peat properties, with *Sphagnum* peat having lower BD, OMBD, C%, N%, and higher C/N ratio than non-*Sphagnum* peat (Figure 6). These differences become important when estimating Holocene peat C fluxes, as the proportion of *Sphagnum*-dominated peat records increases during the late Holocene because of the fen-to-bog transition (Figure 6h). For example, much stronger CH_4 emissions are associated with fens than bogs (e.g. Pelletier et al., 2007). In terms of C sequestration rates, the systematically higher organic C density of non-*Sphagnum* peat suggests that higher accumulation rates are possible in fens than in bogs (Figure 6g), assuming optimal hydroclimatic conditions leading to rapid peat burial. In addition, as non-*Sphagnum* samples contain twice the N mass of *Sphagnum* peat (Figure 6e), early-stage fens have the ability to stock more N than late-stage bogs. Overall, further studies on the timing of the fen-to-bog transition across the northern peatland domain are

needed to better our understanding of its impact on C sequestration and CH_4 emissions.

Holocene pattern of carbon accumulation in northern peatlands

The overall trajectory and shape of our Holocene peat C accumulation curve is similar to the synthesis from a much smaller dataset ($n = 33$; Yu et al., 2009). As such, an early Holocene peak during the Holocene Thermal Maximum (HTM) and an overall slowdown of C accumulation during the mid- and late Holocene, particularly after 4 kyr during the Neoglacial period and associated permafrost development, were found in both syntheses (Figure 7). However, the mean Holocene value of 22.9 ± 2.0 g C/m²/yr (1 SE) presented here is approximately 24% higher than the estimate in Yu et al.'s (2009) study (18.6 g C/m²/yr). Our larger dataset likely better represents the northern peatland C accumulation rates. These results imply that current peat C stocks might be underestimated.

While the peak value at 27 g C/m²/yr is about 23% higher than the time-weighted mean peat C accumulation rate for the remainder of the Holocene at 22 g C/m²/yr, we only found a 2% difference in organic C density values between young (0.053 ± 0.02 g C / cm³) and old (0.057 ± 0.03 g C /cm³) peat samples. These results clearly show that the peak value during the early Holocene cannot be mainly attributed to presumably dense peat deposits that would be rich in recalcitrant C because of long-term decomposition and compaction. Instead, factors influencing the rate of peat burial such as peat type (*Sphagnum* vs non-*Sphagnum* peat; Figure 6), growing season length, and other environmental variables must have been responsible for such high rates of C sequestration during the early Holocene.

The HTM is a well-documented period of orbitally induced warm climate in the northern high-latitude region (Kaufman et al., 2004; Marcott et al., 2013; Renssen et al., 2012) during the early Holocene, caused by maximum summer insolation (Berger and Loutre, 1991; Figure 7a). The peak in warm climatic conditions shows a transgressional pattern across northern North America that moved eastward with the waning Laurentide Ice Sheet during the early and mid-Holocene (Kaufman et al., 2004). This progressive increase in land availability coupled with warming summer conditions have been proposed as the main controls on peatland inception and rapid C accumulation across northern North America (Gorham et al., 2007, 2012; Harden et al., 1992; Jones and Yu, 2010; Yu et al., 2009). In general, our results support the hypothesis that warm summers could promote peat formation and C sequestration (Beilman et al., 2009; Charman et al., 2013; Yu et al., 2009), as the highest rates of C accumulation broadly coincide with the peak in summer insolation from 11 to 7 kyr (Figure 7). We acknowledge that sufficient water input was necessary to allow for peatland development. Furthermore, the observed temporal asymmetry in peatland inception age and peaks in C accumulation rates between Alaska, western Canada, and the Hudson Bay Lowlands follows the transgressional pattern of the HTM. For example, peat inception and highest peat C accumulation rates occur at 11–9 kyr in Alaska, whereas they are delayed in western Canada with peak values around 9–7 kyr. These findings have important implications for projecting the fate of peat C stocks in a future warmer world.

The Neoglacial period is characterized by generally cooler and wetter conditions than the HTM (Figure 7a; Marcott et al., 2013). Particularly low C accumulation rates coincide with this time period across the northern peatland domain (Figure 7; Jones and Yu, 2010; Vitt et al., 2000). Peat accumulation processes might even have stopped in some regions (e.g. Peteet et al., 1998). The onset of permafrost aggradation in many peatlands also occurred during the Neoglacial period (Oksanen et al., 2003; Sannel and Kuhry, 2008; Vitt et al., 2000; Zoltai, 1971, 1995), reducing the

peat C-sink capacity. In addition to shorter and cooler growing seasons, lower C accumulation rates in permafrost sites likely relates to a slower peat burial because of (1) more intense peat decomposition in the acrotelm because of drier surface conditions and (2) a slower rate of peat formation and associated C inputs to soil because many peat plateaus are not *Sphagnum*-dominated. Overall, our results support the notion that climatic changes such as the HTM and the Neoglacial cooling impact C sequestration rates in peatlands.

Role of northern peatlands in the global nitrogen cycle

As relatively few downcore peat N concentrations have been reported in the literature, it was difficult to compare our mean value of 1.2% with previous estimates. Bragazza et al. (2012) reported N content values of 0.7% for *Sphagnum fuscum* litter and 1.48% for *Eriophorum vaginatum* (herbaceous) litter, in line with our results (Table 1). Similarly, Turunen et al. (2004) documented peat N concentrations ranging from 0.35% to 2.25% (mean value of 0.8%) for the uppermost sections of 23 *Sphagnum* bogs across northeastern Canada. Overall, these values closely match our findings for *Sphagnum* (0.7%) and herbaceous (1.7%) peat types (Table 1).

Using our peat C pool estimate of 436 Gt and assuming a mean C/N ratio of 45 yields a peat N pool of 9.7 Gt, roughly equivalent to 10% of the global soil N pool at 95 Gt (Post et al., 1985). This estimate is within the range proposed by Limpens et al. (2006) at 8–15 GtN. The Holocene time-weighted peat N accumulation rate of 0.5 ± 0.04 g N/m^2/yr (SE; Figure 7) is also in line with a previous estimate of 0.19–0.48 g N/m^2/yr (Limpens et al., 2006). While the mid- and late Holocene (6–0 kyr) are characterized by the lowest rates of peat N accumulation at 0.34 g N/m^2/yr, the highest rates (0.61 g N/m^2/yr) occur between 12 and 6 kyr (Figure 7c). The low rates of N accumulation over the past 6 kyr might also relate to the increasing presence and persistence of *Sphagnum* peat (having high C/N ratio and low N concentration) across the northern peatlands (Figures 6 and 7). Overall, given the bias toward *Sphagnum*-dominated sites in our database, N pools and N accumulation rates are probably underestimated.

Rapid N sequestration in peatlands during the early Holocene might have contributed to the global decline in reactive N availability for terrestrial ecosystems (McLauchlan et al., 2013), pointing to a potentially important and undocumented role of northern peatlands in the global N cycle. These results also raise the important question of N provenance: in the absence of large rates of atmospheric N deposition during the early Holocene, the only process that could account for such a large N pool in peatlands is N fixation, either through symbiotic or asymbiotic processes (Limpens et al., 2006).

The fate of these large peat N stocks remains largely unknown under recent and projected warming. Indeed, the importance of peatlands as sources of nitrous oxide (N_2O) is just emerging (e.g. Marushchak et al., 2011; Palmer et al., 2012; Repo et al., 2009), and studies have suggested that reduced surface moisture or increasing temperatures might significantly promote the production, transformation, and transport of dissolved N, and N_2O emissions to the atmosphere through denitrification (e.g. Kane et al., 2010). On the contrary, some authors have speculated that the potential increase in peatland N_2O emissions from climate change may not be significant relative to the global N_2O budget (e.g. Frolking et al., 2011; Martikainen et al., 1993). Overall, additional peat N cycling studies are needed to address these remaining questions.

Future directions

Peat-core analysis has been extensively used over the past 20 years for estimating rates of peat C accumulation at local, regional, and continental scales (e.g. Clymo et al., 1998; Gorham et al., 2012; Mäkilä, 1997; Mäkilä and Saarnisto, 2008; Turunen et al., 2002; Van Bellen et al., 2011; Vitt et al., 2000; Yu et al., 2010). This study analyzed a new database that comprises 268 peat records from 215 northern peatland sites. This systematic analysis of peat properties and Holocene C accumulation rates is essential for accurately addressing the following general research topics in the future: (1) describing and quantifying spatial and temporal patterns of Holocene peatland C and N accumulation, (2) assessing the sensitivity of C and N accumulation to climate change, (3) estimating peatland SOC and soil organic nitrogen (SON) pools at regional and hemispheric scales, (4) furthering our understanding of peatland C cycle–climate linkages, and (5) providing the scientific community with a large dataset for developing and testing earth system and ecological models.

References

Armentano TV and Menges ES (1986) Patterns of change in the carbon balance of organic soil-wetlands of the temperate zone. *Journal of Ecology* 74: 755–774.

Bauer IE, Bhatti JS, Cash KJ et al. (2006) Developing statistical models to estimate the carbon density of organic soils. *Canadian Journal of Soil Science* 86: 295–304.

Beilman DW, MacDonald GM, Smith LC et al. (2009) Carbon accumulation in peatlands of West Siberia over the last 2000 years. *Global Biogeochemical Cycles* 23: GB1012. DOI: 10.1029/2007GB003112.

Belyea LR (2009) Non-linear dynamics of peatlands and potential feedbacks on the climate system. In: Baird A, Belyea L, Comas X et al. (eds) *Northern Peatlands and Carbon Cycling* (American Geophysical Union Monograph Series). Washington, DC: American Geophysical Union, pp. 5–18.

Berger A and Loutre M-F (1991) Insolation values for the climate of the last 10 million years. *Quaternary Science Reviews* 10: 297–317.

Bergner K, Albano Å and Bohlin E (1990) *The Content of Peat: A Compilation of Botanical, Physical and Chemical Data of Peat.* Uppsala: Department of Agricultural Research, Swedish University of Agricultural Sciences.

Björck S and Clemmensen LB (2004) Aeolian sediment in raised bog deposits, Halland, SW Sweden: A new proxy record of Holocene winter storminess in southern Scandinavia? *The Holocene* 14: 677–688.

Blodau C (2002) Carbon cycling in peatlands – A review of processes and controls. *Environmental Reviews* 10: 111–134.

Bragazza L, Buttler A, Habermacher J et al. (2012) High nitrogen deposition alters the decomposition of bog plant litter and reduces carbon accumulation. *Global Change Biology* 18: 1163–1172.

Bridgham SC, Megonigal JP, Keller JK et al. (2006) The carbon balance of North American wetlands. *Wetlands* 26: 889–916.

Cagnon B, Py X, Guillot A et al. (2009) Contributions of hemicellulose, cellulose and lignin to the mass and the porous properties of chars and steam activated carbons from various lignocellulosic precursors. *Bioresource Technology* 100: 292–298.

Camill P (1999) Peat accumulation and succession following permafrost thaw in the boreal peatlands of Manitoba, Canada. *Ecoscience* 6: 592–602.

Chambers FM, Beilman DW and Yu Z (2011) Methods for determining peat humification and for quantifying peat bulk density, organic matter and carbon content for palaeostudies of climate and peatland carbon dynamics. *Mires and Peat* 7: Article 7, 10 pp.

Charman D, Beilman D, Blaauw M et al. (2013) Climate-related changes in peatland carbon accumulation during the last millennium. *Biogeosciences* 10: 929–944. DOI: 10.5194/bg-10-929-2013.

Clymo RS (1984) The limits to peat growth. *Philosophical Transactions of the Royal Society of London. Series B: Biological Sciences* 303: 605–654.

Clymo RS, Turunen J and Tolonen K (1998) Carbon accumulation in peatlands. *Oikos* 81: 368–388.

Dean WE Jr (1974) Determination of carbonate and organic matter in calcareous sediments and sedimentary rocks by loss on ignition: Comparison with other methods. *Journal of Sedimentary Petrology* 44: 242–248.

Frolking S and Roulet NT (2007) Holocene radiative forcing impact of northern peatland carbon accumulation and methane emissions. *Global Change Biology* 13: 1–10.

Frolking S, Talbot J, Jones MC et al. (2011) Peatlands in the Earth's 21st century coupled climate-carbon system. *Environmental Reviews* 19: 371–396.

Glaser PH, Volin JC, Givnish TJ et al. (2012) Carbon and sediment accumulation in the Everglades (USA) during the past 4000 years: Rates, drivers, and sources of error. *Journal of Geophysical Research: Biogeosciences* 117: G03026. DOI: 10.1029/2011JG001821.

Gorham E (1990) Biotic impoverishment in northern peatlands. In: Woodwell GM (ed.) *The Earth in Transition: Patterns and Processes of Biotic Impoverishment*. New York: Cambridge University Press, pp. 65–98.

Gorham E (1991) Northern peatlands: Role in the carbon cycle and probable responses to climatic warming. *Ecological Applications* 1: 182–195.

Gorham E, Lehman C, Dyke A et al. (2007) Temporal and spatial aspects of peatland initiation following deglaciation in North America. *Quaternary Science Reviews* 26: 300–311.

Gorham E, Lehman C, Dyke A et al. (2012) Long-term carbon sequestration in North American peatlands. *Quaternary Science Reviews* 58: 77–82.

Harden JW, Sundquist ET, Stallard RF et al. (1992) Dynamics of soil carbon during deglaciation of the Laurentide ice sheet. *Science* 258: 1921–1924.

Heiri O, Lotter AF and Lemcke G (2001) Loss on ignition as a method for estimating organic and carbonate content in sediments: Reproducibility and comparability of results. *Journal of Paleolimnology* 25: 101–110.

Hughes PDM (2000) A reappraisal of the mechanisms leading to ombrotrophy in British raised mires. *Ecology Letters* 3: 7–9.

Jones MC and Yu Z (2010) Rapid deglacial and early Holocene expansion of peatlands in Alaska. *Proceedings of the National Academy of Sciences U S A* 107: 7347–7352.

Kane ES, Turetsky MR, Harden JW et al. (2010) Seasonal ice and hydrologic controls on dissolved organic carbon and nitrogen concentrations in a boreal-rich fen. *Journal of Geophysical Research: Biogeosciences* 115: G04012. DOI: 10.1029/2010JG001366.

Kaufman DS, Ager TA, Anderson NJ et al. (2004) Holocene thermal maximum in the western Arctic (0–180°W). *Quaternary Science Reviews* 23: 529–560.

Korhola A, Ruppel M, Seppä H et al. (2010) The importance of northern peatland expansion to the late-Holocene rise of atmospheric methane. *Quaternary Science Reviews* 29: 611–617.

Lappalainen E (1996) General review on world peatlands and peat resources. In: Lappalainen E (ed.) *Global Peat Resources*. Jyväskylä: International Peat Society, pp. 53–56.

Limpens J, Heijmans MPD and Berendse F (2006) The nitrogen cycle in boreal peatlands. In: Wieder RK and Vitt DH (eds) *Boreal Peatland Ecosystems* (Ecological Studies, vol. 188). Berlin/Heidelberg: Springer-Verlag, pp. 195–230.

MacDonald GM, Beilman DW, Kremenetski KV et al. (2006) Rapid early development of circum-arctic peatlands and atmospheric CH_4 and CO_2 variations. *Science* 314: 285–288.

McGuire AD, Anderson LG, Christensen TR et al. (2009) Sensitivity of the carbon cycle in the Arctic to climate change. *Ecological Monographs* 79: 523–555.

McLauchlan KK, Williams JJ, Craine JM et al. (2013) Changes in global nitrogen cycling during the Holocene epoch. *Nature* 495: 352–357.

Mäkilä M (1997) Holocene lateral expansion, peat growth and carbon accumulation on Haukkasuo, a raised bog in southeastern Finland. *Boreas* 26: 1–14.

Mäkilä M and Saarnisto M (2008) Carbon accumulation in boreal peatlands during the Holocene – Impacts of climate variations. In: Strack M (ed.) *Peatlands and Climate Change*. Jyväskylä: International Peat Society, pp. 24–43.

Maltby E and Immirzi P (1993) Carbon dynamics in peatlands and other wetland soils, regional and global perspectives. *Chemosphere* 27: 999–1023.

Marcott SA, Shakun JD, Clark PU et al. (2013) A reconstruction of regional and global temperature for the past 11,300 years. *Science* 339: 1198–1201.

Martikainen PJ, Nykänen H, Crill P et al. (1993) Effect of a lowered water-table on nitrous-oxide fluxes from northern peatlands. *Nature* 366: 51–53.

Marushchak ME, Pitkämäki A, Koponen H et al. (2011) Hot spots for nitrous oxide emissions found in different types of permafrost peatlands. *Global Change Biology* 17: 2601–2614.

Mauquoy D and Van Geel B (2007) Mire and peat macros. In: Elias SA (ed.) *Encyclopedia of Quaternary Science*, vol. 3. Amsterdam: Elsevier, pp. 2315–2336.

Oksanen PO, Kuhry P and Alekseeva RN (2003) Holocene development and permafrost history of the Usinsk Mire, northeast European Russia. *Géographie Physique et Quaternaire* 57: 169–187.

Palmer K, Biasi C and Horn MA (2012) Contrasting denitrifier communities relate to contrasting N_2O emission patterns from acidic peat soils in arctic tundra. *The ISME Journal* 6: 1058–1077.

Pelletier L, Moore TR, Roulet NT et al. (2007) Methane fluxes from three peatlands in the La Grande Rivière watershed, James Bay lowland, Canada. *Journal of Geophysical Research: Biogeosciences* 112: G01018. DOI: 10.1029/2006JG000216.

Peteet D, Andreev A, Bardeen W et al. (1998) Long-term Arctic peatland dynamics, vegetation and climate history of the Pur-Taz region, Western Siberia. *Boreas* 27: 115–126.

Piotrowska N, Blaauw M, Mauquoy D et al. (2011) Constructing deposition chronologies for peat deposits using radiocarbon dating. *Mires and Peat* 7: Article 10, 14 pp.

Post WM, Pastor J, Zinke PJ et al. (1985) Global patterns of soil nitrogen storage. *Nature* 317: 613–616.

Reimer PJ, Baillie MGL, Bard E et al. (2009) IntCal09 and Marine09 radiocarbon age calibration curves, 0–50,000 years cal BP. *Radiocarbon* 51: 1111–1150.

Renssen H, Seppä H, Crosta X et al. (2012) Global characterization of the Holocene thermal maximum. *Quaternary Science Reviews* 48: 7–19.

Repo ME, Susiluoto S, Lind SE et al. (2009) Large N_2O emissions from cryoturbated peat soil in tundra. *Nature Geoscience* 2: 189–192.

Ruppel M, Väliranta M, Virtanen T et al. (2013) Postglacial spatiotemporal peatland initiation and lateral expansion dynamics in North America and northern Europe. *The Holocene* 23: 1596–1606.

Rydin H and Jeglum J (2013) *The Biology of Peatlands*. 2nd Edition. Oxford: Oxford University Press, 382 pp.

Sannel ABK and Kuhry P (2008) Long-term stability of permafrost in subarctic peat plateaus, west-central Canada. *The Holocene* 18: 589–601.

Sheng Y, Smith LC, MacDonald GM et al. (2004) A high-resolution GIS-based inventory of the West Siberian peat carbon pool. *Global Biogeochemical Cycles* 18: GB3004. DOI: 10.1029/2003GB002190.

Smith LC, MacDonald GM, Velichko AA et al. (2004) Siberian peatlands a net carbon sink and global methane source since the Early Holocene. *Science* 303: 353–356.

Stolbovoi V (2002) Carbon in Russian soils. *Climatic Change* 55: 131–156.

Stolbovoi V and McCallum I (2002) *Land Resources of Russia*. International Institute for Applied Systems Analysis. Available at: www.iiasa.ac.at/Research/FOR/russia_cd/download.htm.

Stolbovoi V, Montanarella L, Medvedev V et al. (2001) Integration of data on the soils of Russia, Byelorus, Moldova and Ukraine into the Soil Geographic Database of the European Community. *Eurasian Soil Science* 34: 687–703.

Stuiver M and Reimer PJ (1993) Extended ^{14}C database and revised CALIB radiocarbon calibration program. *Radiocarbon* 35: 215–230.

Telford RJ, Heegaard E and Birks HJB (2004) All age-depth models are wrong: But how badly? *Quaternary Science Reviews* 23: 1–5.

Troels-Smith J (1955) Characterization of unconsolidated sediments. *Danmarks Geologiske Undersøgelse Series* 4: 1–73.

Turetsky MR, Wieder RK, Vitt DH et al. (2007) The disappearance of relict permafrost in boreal North America: Effects on peatland carbon storage and fluxes. *Global Change Biology* 13: 1922–1934.

Turunen J, Roulet NT, Moore TR et al. (2004) Nitrogen deposition and increased carbon accumulation in ombrotrophic peatlands in eastern Canada. *Global Biogeochemical Cycles* 18: GB3002. DOI: 10.1029/2003GB002154.

Turunen J, Tomppo E, Tolonen K et al. (2002) Estimating carbon accumulation rates of undrained mires in Finland – Application to boreal and subarctic regions. *The Holocene* 12: 69–80.

Van Bellen S, Dallaire P-L, Garneau M et al. (2011) Quantifying spatial and temporal Holocene carbon accumulation in ombrotrophic peatlands of the Eastmain region, Quebec, Canada. *Global Biogeochemical Cycles* 25: GB2016. DOI: 10.1029/2010GB003877.

Vitt DH, Halsey LA, Bauer IE et al. (2000) Spatial and temporal trends in carbon storage of peatlands of continental western Canada through the Holocene. *Canadian Journal of Earth Sciences* 37: 683–693.

Yu Z (2011) Holocene carbon flux histories of the world's peatlands: Global carbon-cycle implications. *The Holocene* 21: 761–774.

Yu Z (2012) Northern peatland carbon stocks and dynamics: A review. *Biogeosciences* 9: 4071–4085.

Yu Z, Beilman DW and Jones MC (2009) Sensitivity of northern peatland carbon dynamics to Holocene climate change. In: Baird A, Belyea L, Comas X et al. (eds) *Northern Peatlands and Carbon Cycling* (American Geophysical Union Monograph Series). Washington, DC: American Geophysical Union, pp. 55–69.

Yu Z, Campbell ID, Campbell C et al. (2003) Carbon sequestration in western Canadian peat highly sensitive to Holocene wet-dry climate cycles at millennial timescales. *The Holocene* 13: 801–808.

Yu Z, Loisel J, Brosseau DP et al. (2010) Global peatland dynamics since the Last Glacial Maximum. *Geophysical Research Letters* 37: L13402. DOI: 10.1029/2010GL043584.

Yu Z, Loisel J, Turetsky MR et al. (2013) Evidence for elevated emissions from high-latitude wetlands contributing to high atmospheric CH_4 concentration in the early Holocene. *Global Biogeochemical Cycles* 27: 131–140. DOI: 10.1002/GBC.20025.

Zoltai SC (1971) *Southern Limit of Permafrost Features in Peat Landforms, Manitoba and Saskatchewan* (Geological Association of Canada, Special Paper no. 9). St John's, NL: Geological Association of Canada, pp. 305–310.

Zoltai SC (1995) Permafrost distribution in peatlands of west-central Canada during the Holocene warm period 6000 years BP. *Géographie Physique et Quaternaire* 49: 45–54.